THE JOURNAL OF PHYSICAL CHEMISTRY B

Article

pubs.acs.org/JPCB

Excitons in Intact Cells of Photosynthetic Bacteria

Arvi Freiberg,*[,†,‡] Mihkel Pajusalu,[†] and Margus Rätsep[†]

[†]Institute of Physics, University of Tartu, Riia 142, Tartu 51014, Estonia

[‡]Institute of Molecular and Cell Biology, University of Tartu, Riia 23, Tartu 51010, Estonia

ABSTRACT: Live cells and regular crystals seem fundamentally incompatible. Still, effects characteristic to ideal crystals, such as coherent sharing of excitation, have been recently used in many studies to explain the behavior of several photosynthetic complexes, especially the inner workings of the light-harvesting apparatus of the oldest known photosynthetic organisms, the purple bacteria. To this date, there has been no concrete evidence that the same effects are instrumental in real living cells, leaving a possibility that this is an artifact of unnatural study conditions, not a real effect relevant to the biological operation of bacteria. Hereby, we demonstrate survival of collective coherent excitations (excitons) in intact cells of photosynthetic purple bacteria. This is done by using excitation anisotropy spectroscopy for tracking the temperature-dependent evolution of exciton bands in light-harvesting systems of increasing structural complexity. The temperature was gradually raised from 4.5 K to ambient temperature, and the complexity of the systems ranged from detergent-isolated complexes to complete bacterial cells. The results provide conclusive evidence that excitons are indeed one of the key elements contributing to the energetic and dynamic properties of photosynthetic organisms.

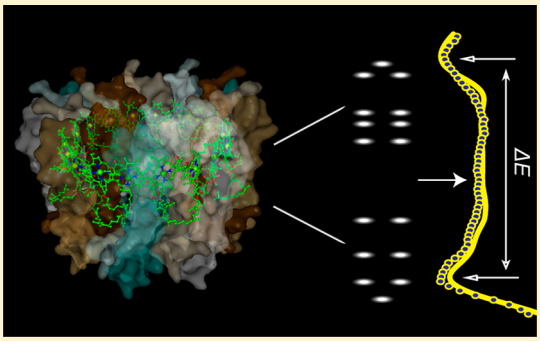

INTRODUCTION

Photosynthesis is one of the most important processes in the biosphere, supplying almost all of the life with energy. Fundamentals of this process, however, lie deep within quantum physics and are still poorly understood.[1−3] One of these quantum-mechanical concepts, nowadays widely used for explaining photosynthesis, is the exciton.[3] An exciton involves collective excitation of many pigment molecules simultaneously, making it possible to transfer energy without any movement of charges. The concept was originally developed theoretically by Frenkel for highly ordered crystals more than eighty years ago.[4] Excitons in the context of photosynthesis have been discussed already since 1938,[5] and exciton effects have been experimentally found in different biological samples that have been cooled to very low temperatures.[3,6] There have been also recent reports about coherent energy pathways in subparts of photosynthetic units at physiological temperatures,[7−9] proving an old theoretical prediction,[10] but still the evidence for excitons within living photosynthetic organisms has remained elusive.

In this paper, we will focus on the presence of excitons within light-harvesting (LH) protein complexes as well as in their functional assemblies from photosynthetic purple bacterium *Rhodobacter (Rb.) sphaeroides*. This species is known to contain highly regular antenna systems,[11] such as LH1 and LH2 complexes, well supporting the exciton idea. The former complexes are naturally found in monomeric and dimeric RC-LH1-PufX configurations consisting of one or two semicircles of bacteriochlorophyll *a* (Bchl) molecules that produce C- and S-shaped B875 antennas around, respectively, one or two reaction centers (RC)[12−14] (see Figure 1 for a dimeric RC-LH1-PufX structure). The LH2 complex consists of two arrays of Bchl molecules in circular arrangement, one of them (B800 in Figure 1), close to the cytoplasmic side of the protein, contains nine, and the other (B850), at the periplasmic side, eighteen molecules.[15] Both the RC-LH1-PufX and LH2 complexes self-assemble into intracytoplasmic membrane vesicles (chromatophores) within the bacterial cytoplasm.[16,17] The solar radiation itself is absorbed by the antenna pigments, and the excitation energy is funneled to the RC, where it is efficiently utilized in a sequence of electron transfer processes.[18,19] To verify generality of the results, parallel measurements were also conducted on samples from *Rhodopseudomonas (Rps.) acidophila*, another photosynthetic purple bacterium, whose LH complexes are similar to those of *Rb. sphaeroides*.[15,20]

The present work was primarily designed to identify the physiological-temperature exciton effects in LH complexes under conditions of different complexity, both in detergent-isolated and in natural, membrane-bound, forms. To systematically study this problem, we begin by characterizing the spectral properties of the individual complexes in the most easily interpretable cases, which are solidified solutions of detergent-isolated complexes at near absolute-zero temperature

Special Issue: Rienk van Grondelle Festschrift

Received: October 5, 2012
Revised: January 9, 2013

   dx.doi.org/10.1021/jp3098523 | *J. Phys. Chem. B* XXXX, XXX, XXX−XXX

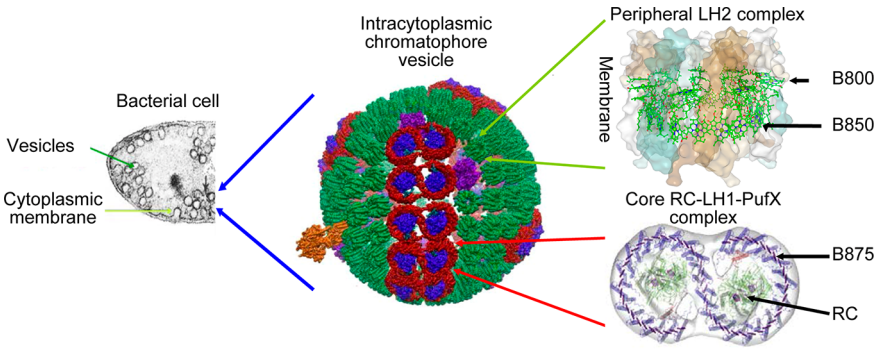

Figure 1. Overall architecture of the intracytoplasmic chromatophore vesicle[17] from the wild type strain of purple bacterium *Rb. sphaeroides* and its constituent parts: peripheral LH2[2,20] and dimeric core RC-LH1-PufX protein complexes.[14] B800, B850, and B875 denote assemblies of Bchl molecules in the LH2 and LH1 complexes.

of 4.5 K. Then, the same features will be tracked as a function of temperature between 4.5 and 290 K, as degrees of structural complexity are added. In the order of increasing complexity, these samples include: buffer solutions of mutant membranes, containing only single type (either RC-LH1-PufX or LH2) of complexes; a solution of functional membrane vesicles, complete with both RC-LH1-PufX and LH2 complexes; and a suspension of bacterial cells.

Foremost, the tightly packed B850 and B875 pigment configurations in, respectively, LH2 and LH1 antennae support the idea of excitons.[3] The availability of high-resolution structural data of LH2 complexes has made it possible to study exciton interactions within the B850 ring thoroughly, contributing to a detailed understanding of its optical properties (see refs 6 and 21−25 for reviews). The 18 Bchl pigments of the system are arranged into two interspaced C_9 symmetrical rings.[20] Interactions between the transition dipole moments of the lowest-energy (Q_y) molecular transitions split the resulting 18 exciton states energetically into a broad band schematically shown in Figure 2a. Under ideal conditions, most of these states are unfavorable for absorption because their dipole moments are small; therefore, the optical properties of B850 are mainly determined by the exciton band edge states indexed as the $k = \pm1$ and $k = \pm8$ states. In the presence of static[26,27] and dynamic[25,28,29] disorders that arise, respectively, from different local environments (inhomogeneous broadening) and from coupling of excitons to the phonon bath (homogeneous broadening), the remaining degeneracy between exciton states vanishes. In large ensembles of LH2 complexes, a virtually continuous distribution of exciton states is formed, as demonstrated in Figure 2b. Although the disorders release strict optical selection rules the general circular geometry of the Bchl sites determines that majority of the transition dipole moment is concentrated into the $k = \pm1$ states at the low-energy exciton band edge, which shape the characteristic B850 absorption band of LH2. A minor amount of the dipole moment is also distributed to the $k = \pm8$ states in the opposite, high-energy side of the exciton state manifold. The respective absorption peak is, however, very weak and hard to observe in steady-state experiments due to overlap with other absorbing components such as the B800 chromophores or trace Bchls. At a sufficiently strong exciton−phonon bath coupling the original exciton states may rapidly localize into self-trapped (ST) exciton states.[30] This process is promoted by inhomogeneous broadening.[31,32] Consequently, at low temperatures, the energy absorbed by any of the absorbing states propagates to the

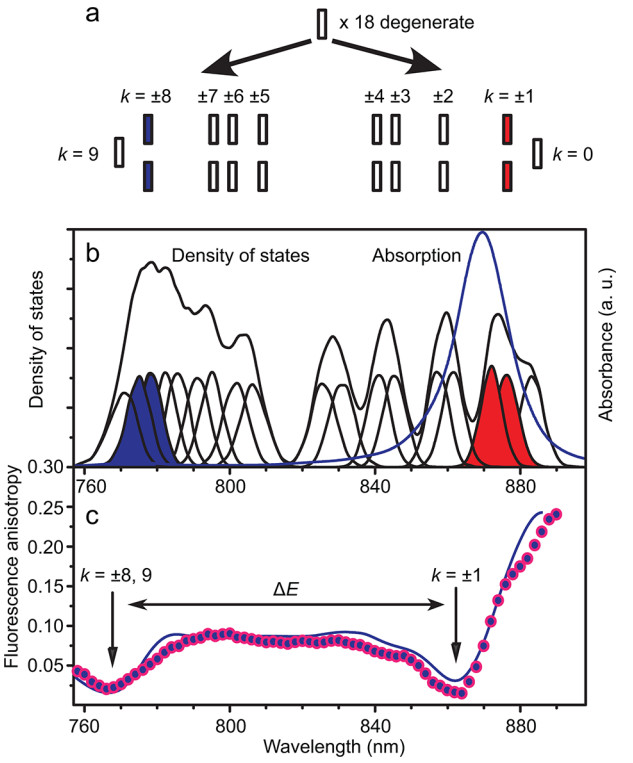

Figure 2. Spectroscopic features of the B850 ring (modeled for LH2 from *Rps. acidophila*).[34] (a) In a perfectly ordered B850 ring, resonant couplings between the transition dipole moments of Bchl molecules cause a manifold of 18 Frenkel exciton states, indexed from $k = 0$ to $k = 9$, to form a band. Sixteen of these states are shown to be pairwise energetically degenerate. The edge degenerate states at the top and bottom of the exciton band are in blue and red, respectively. (b) Modeled distribution of the exciton states, when static disorder is applied. Most of the dipole strength is concentrated in $k = \pm1$ region (red), explaining the essence of the B850 absorption band (blue line). (c) Experimental (scatter) and modeled (solid line) fluorescence excitation anisotropy spectrum at 4.5 K. The locations of the main anisotropy minimums are marked with arrows; denoted also are the exciton states dominant in their formation. Energy difference between the minimums, indicated as ΔE, provides a measure of the exciton bandwidth.

lowest ST exciton state and both energy transfer and fluorescence are facilitated by that state.[33] At higher temperatures, the participation of high-energy ST states in emission

dx.doi.org/10.1021/jp3098523 | J. Phys. Chem. B XXXX, XXX, XXX−XXX

Table 1. Buffers and Detergents Used for Preparing Measurement Samples from *Rb. sphaeroides* and *Rps. acidophila*

complex	buffer	detergent
	Rb. sphaeroides	
LH2 isolated	TEN (15 mM Tris−HCl pH 8.0, 1 mM EDTA, 0.1 M NaCl)	1% LDAO
LH2 membrane	TEN (15 mM Tris−HCl pH 8.0, 1 mM EDTA, 0.1 M NaCl)	NA[a]
RC-LH1-PufX isolated	20 mM HEPES pH 7.8	0.03% β-DDM
RC-LH1-PufX membrane	20 mM HEPES pH 7.8	NA[a]
Cells	20 mM Tris pH 7.5	NA[a]
Full membranes	TEN (15 mM Tris−HCl pH 8.0, 1 mM EDTA, 0.1 M NaCl)	NA[a]
	Rps. acidophila	
Full membrane	20 mM Tris pH 8.0	NA[a]
LH2 isolated	TEN (15 mM Tris−HCl pH 8.0, 1 mM EDTA, 0.1 M NaCl)	3% LDAO

[a]NA - not applicable.

and energy transfer become important due to phonon-assisted transitions.[34]

The fluorescence excitation anisotropy spectroscopy is the main method employed in the current study, because it gives a possibility of distinguishing the band-edge exciton states in the cyclic bacterial LH complexes. This was first experimentally demonstrated in ref 35 for the LH2 and B800 deficient LH2 complexes of *Rb. sphaeroides* and theoretically substantiated in ref 36. Subsequently, LH1[37] complexes from *Rb. sphaeroides* and LH2[34] and LH3[34] complexes from *Rps. acidophila* have also been studied by this method. The current model to analyze fluorescence anisotropy spectra of excitons in the B850 ring of LH2 was presented[34] and will not be repeated in any detail here. It is based on an assumption that photons are absorbed by a set of Frenkel exciton states, which, due to exciton−phonon coupling, promptly relax into a ST state of lower energy. Due to this energy-stabilizing process, which is accompanied by lattice deformation,[30] the directions of the transition dipole moments of the absorbing and emitting states generally differ, offering a chance to differentiate between specific exciton states via fluorescence excitation anisotropy spectroscopy. The anisotropy $r(\lambda)$ represents a weighted average of a function of the angles α_k between the dipole moments of the kth absorbing exciton states and emitting ST exciton states when the sample is excited with a monochromatic light source at wavelength λ:

$$r(\lambda) = \left\langle \frac{3\cos\alpha_k - 1}{5} \right\rangle_k = \frac{I_{vv}(\lambda) - I_{vh}(\lambda)}{I_{vv}(\lambda) - 2I_{vh}(\lambda)} \quad (1)$$

When the transition dipole moments of the absorbing and emitting states are predominantly parallel, such as for the states at the low-energy band edge, the anisotropy is high (the limiting value for strictly parallel dipoles is 0.4). On the other hand, low anisotropy signifies largely perpendicular dipole moments, −0.2 being the limiting value when the dipoles are perpendicular to each other. According to eq 1, the anisotropy can be measured by using a linearly polarized monochromatic light source to excite the sample and by integrating the emission spectra collected through two polarizers: one ($I_{vv}(\lambda)$) polarized in parallel to and second ($I_{vh}(\lambda)$) polarized perpendicularly to the polarization of the excitation light beam.

As an example, in Figure 2c, an experimental anisotropy spectrum of LH2 complexes from *Rps. acidophila*, recorded at 4.5 K,[34] is presented in parallel with a simulated spectrum. It can be seen that both experiment and theory clearly identify two low-anisotropy dips, one at the low-energy edge and another at the high-energy edge of the exciton state manifold. Similar good agreement between experiment and theory has been achieved upon raising temperature up to physiological temperatures. A theoretical analysis provided in refs 25, 34, and 38 shows that the low-energy dip is primarily related to the $k = \pm 1$ exciton states, whereas the one at higher energies corresponds to the $k = \pm 8$ and $k = 9$ states. It was also shown that the energy difference ΔE between the anisotropy dips provides a fair measure for the width of the exciton state manifold (exciton bandwidth for short). This former knowledge is used in the following to find the signatures of the band edge states in light-harvesting systems of increasing complexity. Identifying the dips in the anisotropy spectra of full membranes and cells at physiological temperatures first proves the existence of coherent light excitations in functional photosynthetic organisms.

MATERIALS AND METHODS

Samples. The purified into detergent micelles and self-assembled into native photosynthetic membranes LH complexes from wild type (WT) *Rb. sphaeroides* (strain 2.4.1) and *Rps. acidophila* (strain 10050) were prepared as described earlier.[39,40] Cultures of a *Rb. sphaeroides* strain with deleted antenna or RC genes (of which the RC-LH1-PufX and LH2-only membrane samples were obtained) were grown semi-aerobically in a nutrient rich medium. During the final preparations the samples were diluted with corresponding buffer solutions and detergents were added to samples with isolated complexes to keep the LH complexes isolated from each other (see Table 1 for exact buffer and detergent combinations per sample). Bacterial cell samples were grown for 24 h in photosynthetic conditions, after which the cell development was halted. The cells were later diluted to achieve a sufficiently low optical density.

All of the samples were diluted with glycerol (1:2 volume ratio) to get transparent glassy samples when freezing. Adding glycerol slightly stabilizes (red-shifts) the spectra of preparations from *Rb. sphaeroides*, but practically does not influence the spectra of those from *Rps. acidophila*.[40] Gelatin capsules of 4 mm diameter were used as sample containers during measurements.

Conventional Absorption-Fluorescence Spectroscopy. The spectroscopy setup available in our laboratory for absorption/fluorescence emission measurements has been recently described.[40] The wavelength scale of the spectrometer was determined with a precision of ±0.1 nm by using a Ne−Ar calibration lamp. Measurements at low temperatures were performed in a liquid helium cryostat (Utreks, Ukraine), equipped with a temperature control system that stabilizes the temperature within ±0.2 K. The temperature dependences

dx.doi.org/10.1021/jp3098523 | J. Phys. Chem. B XXXX, XXX, XXX−XXX

were measured from lower to higher temperatures starting from 4.5 K.

Polarized Fluorescence Excitation Spectroscopy. The fluorescence spectra were collected by exciting the sample with a continuous-wave Ti: sapphire laser (Spectra Physics). A reference channel was used to correct the fluorescence spectra for the effect of laser intensity fluctuations. The sample fluorescence was viewed at 90° geometry with respect to the excitation beam. For anisotropy measurements the emitted light path was equipped with two interchangeable polarizers, one polarized in parallel to the exciting laser's polarization and another polarized perpendicularly to it. The fluorescence spectra were recorded using an Andor (GB) Shamrock 303i spectrometer equipped with a CCD camera. To eliminate polarization sensitivity of the monochromator and the CCD array, the wavelength-sensitivity curves were measured for both polarizers using a nonpolarized light source. In creating the anisotropy spectrum, either the total fluorescence spectrum or its spectrally selected parts were integrated together, depending on the task.

Scattering of light in the sample and from the elements of the measuring system is the foremost source of possible artifacts in anisotropy measurements. An unpolarized component added to the polarized signal can produce distortions of the anisotropy spectrum calculated according to eq 1, because the unpolarized part would be canceled in the numerator, but not in the denominator. Because the scattering intensity increases in correlation with absorbed energy, this effect would be expected to produce anisotropy dips very close to absorption maxima. Therefore, all of the anisotropy features in this work have been scrutinized to find their origin. Given the very weak anisotropy features recorded at ambient temperatures (see below), their authenticity has been proven by following the evolution of the anisotropy spectra from low temperatures (where all the relevant signals are appreciably strong) to ambient temperatures, as well by repeating the measurements a number of times.

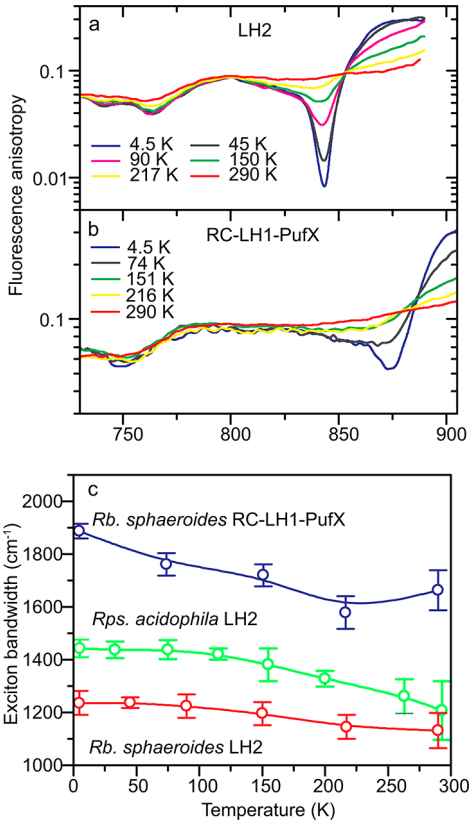

Figure 3. Temperature dependence of the fluorescence excitation anisotropy spectra of detergent-isolated LH2 (a) and LH1-RC-PufX (b) complexes from *Rb. sphaeroides*, and of the exciton bandwidth (c) for the same complexes (blue and red data points) as well as for the LH2 complex from *Rps. acidophila* (green). Please notice the logarithmic vertical scale used in (a) and (b) panels to amplify weak signal parts. The lines in panel (c) are merely for leading the eye. Error bars denote estimate standard deviation of regression used to determine the anisotropy minima.

RESULTS AND DISCUSSION

Detergent-Isolated Complexes. The fluorescence excitation anisotropy spectra of purified peripheral LH2 and core RC-LH1-PufX antenna complexes from *Rb. sphaeroides*, recorded at different temperatures between 4.5 and 290 K, are shown in Figure 3 (parts a and b). In agreement with the previous studies,[35,37] the low-temperature spectra of both types of complexes contain similar spectral features: a deep long-wavelength dip, a shallow short-wavelength dip, and a rising slope at longer wavelengths. As indicated above, the dips correspond to higher- and lower-energy extremes of the exciton band states. From the separation of the dips, it is evident that the exciton band in core complexes is broader than in peripheral complexes. The anisotropy rise in the low-energy region is in both types of complexes produced by absorption of the $k = 0$ states at the red edge of respective absorption spectra depicted in Figure 4. Worth noticing also is the absence in the LH2 spectra of any anisotropy feature that could be related to the strong B800 absorption band. Evidently, the photons absorbed directly by the B800 chromophores lose almost totally their polarization "memory" in the process of excitation transfer from B800 to the fluorescing B850 exciton system.

Temperature dependences of the anisotropy spectra also appear similar in the case of both complexes. With increasing temperature the minima decrease in depth and widen, while their positions shift toward each other. Notable is the greater thermal sensitivity of the low-energy dip, causing its virtual disappearance from the spectrum at ambient temperatures. Increased activity of nuclear vibrations, and associated phonon-assisted mixing and occupation of the higher-energy emitting exciton states, may be responsible for these spectral modifications.[25,34] Because the high-energy dip in the anisotropy spectra is invariably present over the whole temperature range, it is evident that excitons in all the studied LH complexes survive the rise of temperature to physiological levels. Correlated thermal shifts and broadenings are also observed in the absorption spectra of the complexes (Figure 4). However, as already commented above, the absorbance around 750−770 nm, particularly at elevated temperatures, is too weak and indecisively structureless for determination the position of the high-energy exciton band edge.

Figure 3c depicts the temperature dependence of the exciton bandwidth ΔE, as defined in Figure 2c, for LH2 and RC-LH1-PufX complexes from *Rb. sphaeroides* and LH2 complexes from *Rps. acidophila*. Observed in the LH2 complexes from *Rb. sphaeroides* is just a minor ∼8% shrinkage of the bandwidth, from 1236 cm^{-1} at 4.5 K to 1132 cm^{-1} at 290 K, when going from deep cryogenic to physiological temperatures. In LH2 from *Rps. acidophila* the decrease is twice as large, reaching ∼16% (from 1442 to 1207 cm^{-1}). Similar temperature

dx.doi.org/10.1021/jp3098523 | J. Phys. Chem. B XXXX, XXX, XXX−XXX

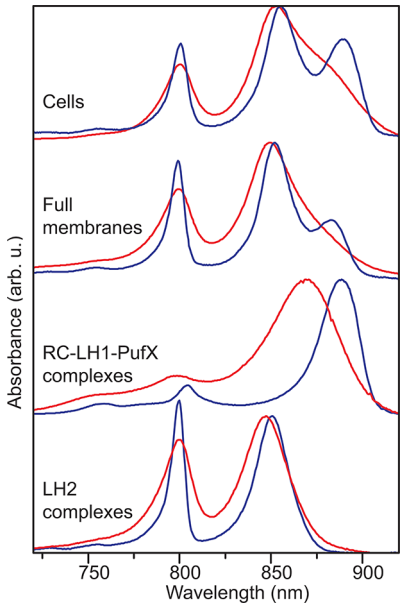

Figure 4. Comparison of the absorption spectra of *Rb. sphaeroides* cells with the spectra of chromatophore membranes and isolated LH2 and RC-LH1-PufX complexes from the same species at 4.5 K (blue) and ambient temperature (red). The spectra are normalized according to the main absorption maximum. The positions of the B850 and B875 exciton bands at 850 and 875 nm, respectively, demonstrate high sensitivity to temperature, whereas the position of the B800 band at 800 nm, related to quasi-localized excitations of quasi-monomeric Bchl molecules is rather temperature insensitive.

dependences in the case of LH2 were revealed in refs 41 and 42 by using other methods, albeit with slight differences in the absolute values of the bandwidth. As was known already previously,[35,37] the exciton bandwidth in core complexes is almost 50% broader than in peripheral complexes. In RC-LH1-PufX complexes from *Rb. sphaeroides* the bandwidth shrinks with temperature by ~12% (from 1887 to 1663 cm^{-1}).

Native Membrane-Assembled Complexes. In nature, the antenna complexes are crowded into photosynthetic membrane vesicles, as demonstrated in Figure 1. Tight packing is required for efficient intercomplex excitation energy transfer, to secure high quantum yield of solar energy harvesting. The excitation energy transfer, taking place along the membrane surface, inevitably disturbs the phase relationships between the absorbing and emitting states. In the anisotropy spectra this must lead to further shallowing or even complete disappearance of the anisotropy minima.

To investigate the influence of energy transfer on the fluorescence excitation anisotropy spectra in the simplest case, the mutant membranes that include just one type of the complexes, either LH2 or RC-LH1-PufX, were studied. Previous measurements have demonstrated active intercomplex energy transfer in these single-component membranes.[40,43,44] It can be seen in Figure 5 that, at least at low temperatures, general features of the anisotropy spectra of the complexes survive the packing into membrane environment. The most notable difference, compared to the spectra of isolated complexes, is the reduced and broader low-energy dip. This is rather expected for the conditions of intercomplex energy transfer, as discussed above.

Because the dip positions change only slightly subsequent to assembly into membrane, the exciton properties in isolated and

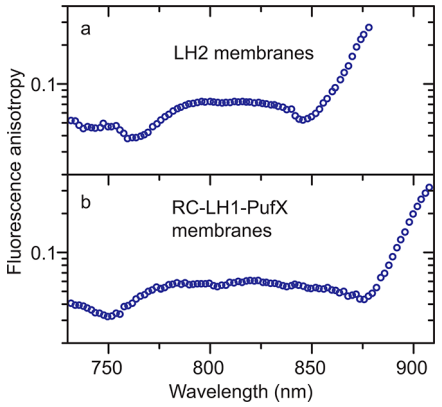

Figure 5. Fluorescence anisotropy excitation spectra of mutant LH2-only (a) and RC-LH1-PufX-only (b) membranes of *Rb. sphaeroides* at 4.5 K.

membrane complexes must be rather similar. Still, exact comparison of the bandwidths presented in Table 2 reveals that the bandwidths in membranes are invariably greater than in isolated complexes. This is again in fair agreement with the previously known spectroscopic data for purified and membrane-embedded complexes.[35,38,40]

Full Membranes Complete with LH2 and RC-LH1-PufX Complexes and Intact Cells. We further consider chromatophores and cells of *Rb. sphaeroides* that include all the components of photosynthetic machinery and energy transfer pathways.[16] At least at low temperatures, the anisotropy spectra of these systems, recorded by integrating over the whole fluorescence spectrum, seem to feature some combination of the properties of individual LH complexes. The spectra shown in Figure 6 present three shallow minima that obviously correspond to the dips in the spectra of LH2 and RC-LH1-PufX membrane complexes. An overlap of the LH2 and RC-LH1-PufX spectra at short wavelengths results in a single, broad high-energy minimum around 750−775 nm. Increasing the temperature broadens the spectra and reduces their structure. Yet the high-energy minimum remains clearly observable at 290 K, implying that even in those most intact structures the antenna excitons might be present under physiological conditions. Although the spectra of chromatophores and cells are qualitatively very similar both at low and at high temperatures, the cell spectra are noisier and less structured. This is understandably the result of enhanced excitation light scattering efficiency of the cell sample.

The measurements conducted on the samples from *Rps. acidophila* (Figure 7) produce similar but not identical results with the samples from *Rb. sphaeroides*. In the case of isolated LH2 complexes (Figure 7a) the main difference concerns the high-energy dip, which is much deeper in the complexes from *Rps. acidophila*. In the chromatophores from *Rps. acidophila* (Figure 7b), on the other hand, the low-energy dip corresponding to LH2 is indistinguishable, whereas in *Rb. sphaeroides* (Figure 6a) it is clearly visible. We shall return to these subtleties at the end of this part of the article.

It is noticeable that in chromatophores and cells, like in purified samples containing LH2 complexes, there is no anisotropy dip related to the strong absorption of the B800 BChls enclosed in LH2. It was above suggested that loss of polarization of the absorbed photons in the process of excitation transfer effectively smears out this feature. Because energy transfer is the major antenna function in photosynthetic

dx.doi.org/10.1021/jp3098523 | J. Phys. Chem. B XXXX, XXX, XXX−XXX

Table 2. Bandwidths of Excitons in Detergent-Isolated and Membrane-Embedded Light-Harvesting Complexes from *Rb. sphaeroides* and *Rps. acidophila* at 4.5 K

			dips in the spectrum		
	sample		high-energy (nm)	low-energy (nm)	bandwidth[a] with standard deviation of regression (cm^{-1})
Rb. sphaeroides	LH2	complex	763.1	842.6	1236(21)
		membrane	763.2	845.8	1279(9)
	LH1[b]	complex	755.7	880.1	1871(31)
		membrane	749.6	882.8	2013(22)
	RC-LH1[b]	complex	751.8	880.1	1939(39)
		membrane	751.1	880.4	1955(20)
	RC-LH1-PufX	complex	749.8	873.3	1886(28)
		membrane	751.5	869.5	1892(22)
Rps. acidophila	LH2	complex	766.5	861.7	1442(13)
		membrane[c]	765.8	863.1	1473(27)
	LH1	complex[d]	N/A	N/A	N/A
		membrane[c]	765.6	901.6	1969(15)

[a]Defined as the energy difference between the high-energy dip of the polarized fluorescence excitation spectrum and the low-energy dip. [b]From ref 37. [c]Obtained from WT membrane spectra by integrating only the corresponding (LH1 or LH2) emission regions. [d]N/A - not available.

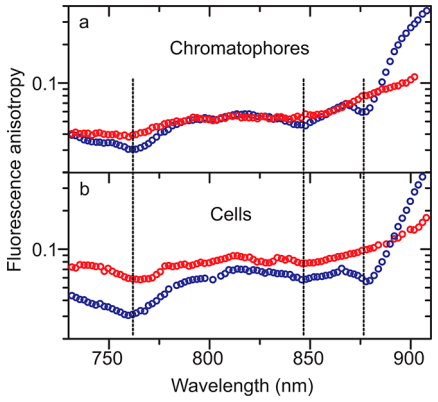

Figure 6. Fluorescence anisotropy excitation spectra of chromatophores (a) and cells (b) of *Rb. sphaeroides* measured at 4.5 K (blue) and 290 K (red) by integrating over the whole fluorescence spectrum. The minima corresponding to LH1-RC-PufX and LH2 complexes are marked with vertical dashed lines.

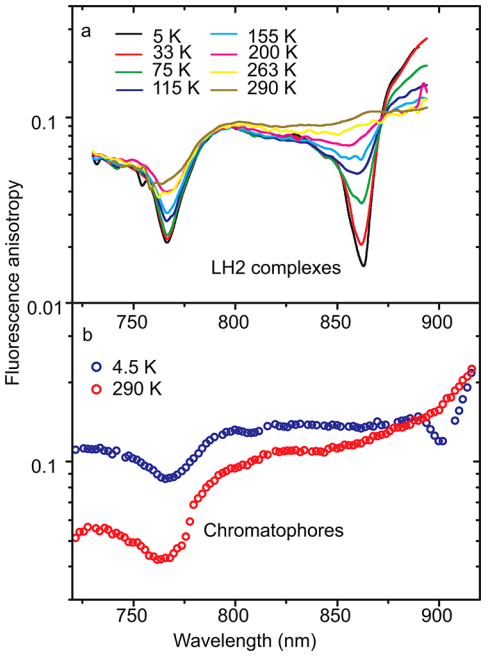

Figure 7. Temperature dependence of the fluorescence anisotropy excitation spectra of isolated LH2 complexes (a) and chromatophores (b) from *Rps. acidophila* at 4.5 K (blue) and 290 K (red). The spectra are measured by integrating over the whole fluorescence spectrum.

membranes, the apparently additive character of the spectra corresponding to core and peripheral antenna excitons in the fluorescence anisotropy spectra of chromatophores and cells requires explanation. The confusion mostly concerns the visibility in Figure 6 of the low-energy anisotropy dips related to B850 excitons. However, this puzzlement can be easily rationalized by the known structural and functional heterogeneity of antenna complexes in the photosynthetic purple bacteria. As was established in ref 45, along with perfectly assembled and well-functioning LH2-RC-LH1-PufX photosynthetic units, the chromatophores may also contain the LH2-only domains (as well as lone LH2 complexes) with strongly impaired excitation energy transfer to the core complexes.[38,46] These peripheral antenna structures develop late in the membrane remodeling process, during adaptation to the growth illumination conditions, and correlate with the extent of the observed fluorescence heterogeneity.[16] The chromatophores (and cells) studied in this work are without a doubt heterogeneous in the above sense. This is confirmed by the peculiar shape of the low-temperature fluorescence spectra presented in the insets of Figure 8. Apart from the main emission band related to core complexes, they acquire strong shoulders from the high energy side. Responsible for these shoulders are the LH2 complexes detached from the ultrafast LH2 to core energy transfer pathways; otherwise, it would not be present.[38,46]

To further elucidate the effects of fluorescence heterogeneity on the anisotropy spectra of chromatophores and cells, the spectra corresponding to fluorescence from selected spectral ranges were presented. As demonstrated in Figure 8, this way drastic dependence of the anisotropy spectra on the fluorescence integration range is revealed. When the fluorescence is collected in the LH2 emission range (red data), the anisotropy spectrum reminds that of the LH2-only membranes or, especially in the case of *Rb. sphaeroides*, rather a mixture of LH2-only membranes and isolated LH2 complexes. On the other hand, when the direct LH2 emission is properly screened by recording fluorescence only in long-wavelength

dx.doi.org/10.1021/jp3098523 | J. Phys. Chem. B XXXX, XXX, XXX−XXX

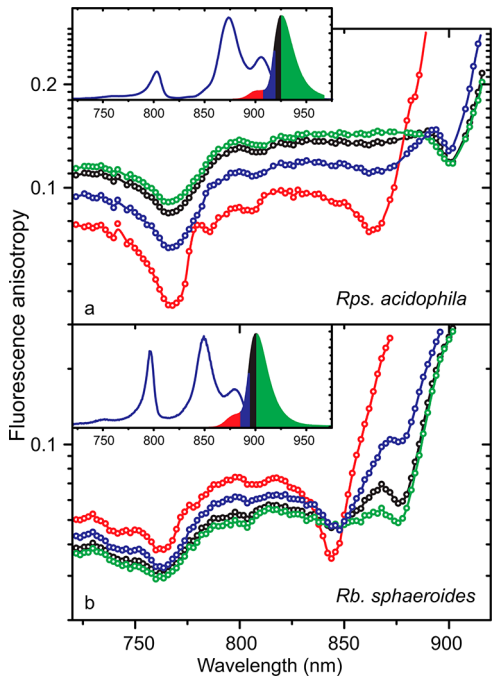

Figure 8. Dependence of the fluorescence anisotropy excitation spectra of the chromatophores from *Rps. acidophila* (a) and *Rb. sphaeroides* (b) on the fluorescence recording range. The colored data points are obtained by integrating fluorescence over the filled areas of corresponding color shown in the insets. The black color data are obtained by integration over the whole fluorescence band. A similar color code is used in both panels. Shown with blue line in the insets are absorption spectra. The lines connecting data points are to lead the eye. See text for further details.

range (green data), the anisotropy spectrum is (mostly) related to core complexes. Recording the fluorescence in the intermediate range, which involves independent emission from peripheral as well as from core antennas, also shows strong response from both these antennas (blue data). Integrating over the whole emission range (black data), as was done so far, in principle exposes signals from all types of directly excited LH complexes. Now the LH2 feature (around 866 nm in *Rps. acidophila* and 846 nm in *Rb. sphaeroides*) appears smaller than that in the blue spectrum, in correlation with the diminished LH2 and LH1 fluorescence intensity ratio.

Worth noticing as well in Figure 8 is the fact that the high-energy limits of the exciton state manifolds in the core and peripheral antenna complexes are tuned together, so that the broader LH1 exciton band totally engulfs the narrower LH2 band. In the LH2-only and RC-LH1-PufX-only membranes the locations of the corresponding dips clearly vary (Figure 5). It seems plausible that during the assembly process of native membranes the antenna proteins acquire different conformation from that they have in mutant membranes. Such adaptation mostly concerns core antennas, because the LH2 exciton parameters change very little. This is quite understandable, given the open, thus more flexible, structural shape of the LH1 complexes (see Introduction). The great overlap of the LH1 and LH2 exciton states is most probably not accidental. Rather, it is required for ultrafast excitation energy transfer within the antenna. These processes are observed to take place in the 1−10 ps time range.[3,47−50] A significant role of dark exciton states in securing efficient exciton transfer in multichromophoric systems has been emphasized.[22,51]

Let us finally briefly discuss the most notable difference between the fluorescence anisotropy spectra of full membranes from *Rps. acidophila* and *Rb. sphaeroides*. It ought to be quite evident from the preceding presentation that the samples from *Rps. acidophila* should be structurally more homogeneous than those from *Rb. sphaeroides*. As can be seen from Figure 8b, in the latter case, it is practically impossible to get rid from the spurious LH2 signal by merely selecting the fluorescence recording range, suggesting a very broad spectral coverage of LH2 complexes in this sample. Indeed, it was previously shown[40] that the LH2 fluorescence can be excited even past 900 nm, deep in the LH1 fluorescence range, which explains the observation. The dissimilarity of the anisotropy spectra of isolated LH2 complexes from the two bacterial species once again points to their possible structural differences, frequently noted in the literature.[15,20,52]

CONCLUSIONS

In this work, the fate of excitons in bacterial LH complexes is studied, following assembly into more complex systems, toward the whole functioning cells at ambient temperatures. Our results show conclusively that the exciton band structure, thus the superposition of molecular states as well as fair amount of phase memory between these states, manages to survive in the fully developed cells of photosynthetic bacteria. Because parallel considerations hold for the samples from two different species, we are confident that excitons at functional temperatures are generic for all photosynthetic (purple) bacteria.

This is quite remarkable because, apart from the considerable cellular structural disorder, the temperature is supposed to induce essential decoherence of the states that at the limit of $\lambda \gg V$ (where λ is the protein reorganization energy and V is the exciton coupling energy) would lead to decoupling of the cofactors and destruction of the excitons. A straightforward, though crude, estimate ($V \approx \Delta E/4$) of the nearest neighbor coupling energy at room temperature yields $V \approx 302$ cm^{-1} for the LH2 excitons from *Rps. acidophila* and $V \approx 283$ cm^{-1} for *Rb. sphaeroides*. Both these numbers are significantly less than the corresponding λ ($\lambda = 358$ cm^{-1} was estimated for excitons in LH2 from *Rps. acidophila*[34]). Proposals have been made that the protein scaffold is someway special in protecting electronic state coherences.[53,54] According to another idea[55] the common relationship between V and λ is only valid when the system is in thermal equilibrium with its environment. In the opposite case, the temperature no longer provides a relevant energy scale against which to compare the quantum behavior of the system. This role is taken over by an effective temperature, which can be much lower than the absolute temperature. The similar magnitudes of the electronic and exciton-lattice coupling energies imply that exciton processes in LH antennas might indeed take place in nonequilibrium conditions, partly explaining the above conundrum.

Although full biological relevance of excitons remains to be understood, benefits of excitons as solar energy carriers in photosynthesis are rather obvious. First, exciton spectra are relatively simply tunable, making it possible to adapt to different illumination conditions. An example of such adaptation in the case of *Rps. acidophila* is discussed in ref 38. Second, excitons provide extremely large spectral coverage (≥2000 cm^{-1}, Table 2) of radiation collection, which would be difficult to achieve otherwise. Third, as evidenced by this study, excitons are very robust against various environmental disorders, including those induced by temperature, which in

dx.doi.org/10.1021/jp3098523 | J. Phys. Chem. B XXXX, XXX, XXX−XXX

the case of localized excitation would easily obliterate functional energy transfer pathways.

AUTHOR INFORMATION

Corresponding Author

*Phone: +372 5645 3175. E-mail: arvi.freiberg@ut.ee.

Notes

The authors declare no competing financial interest.

ACKNOWLEDGMENTS

Estonian Research Council (Grant IUT02-28) supported this work. It was also partially supported by the graduate school, "Functional materials and technologies", receiving funding from the European Social Fund under project 1.2.0401.09-0079 in Estonia. The authors are grateful to R. Cogdell, T. Gillbro, N. Hunter, R. Niederman, and N. Woodbury for generously donating the samples.

REFERENCES

(1) Markvart, T. *Progr. Quantum Electron.* **2000**, *24*, 107−186.
(2) *Photosynthesis in Silico. Understanding Complexity From Molecules to Ecosystems*; Laisk, A., Nedbal, L., Govindjee, Eds.; Springer: Heidelberg, 2009.
(3) Van Amerongen, H.; Valkunas, L.; Van Grondelle, R. *Photosynthetic Excitons*; World Scientific: Singapore, 2000.
(4) Frenkel, J. *Phys. Rev.* **1931**, *37*, 1276−1294.
(5) Franck, J.; Teller, E. *J. Chem. Phys.* **1938**, *6*, 861−872.
(6) Cogdell, R. J.; Gall, A.; Köhler, J. *Q. Rev. Biophys.* **2006**, *39*, 227−324.
(7) Harel, E.; Engel, G. S. *Proc. Natl. Acad. Sci. U. S. A.* **2012**, *109*, 707−711.
(8) Panitchayangkoon, G.; Voronine, D. V.; Abramavicius, D.; Caram, J. R.; Lewis, N. H. C.; Mukamel, S.; Engel, G. S. *Proc. Natl. Acad. Sci. U. S. A.* **2011**, *108*, 20909−20912.
(9) Panitchayangkoon, G.; Hayes, D.; Fransted, K. A.; Caram, J. R.; Harel, E.; Wen, J.; Blankenship, R. E.; Engel, G. S. *Proc. Natl. Acad. Sci. U. S. A.* **2010**, *107*, 12766−12770.
(10) Nedbal, L.; Szöcs, V. *J. Theor. Biol.* **1986**, *120*, 411−418.
(11) *Anoxygenic Photosynthetic Bacteria*; Blankenship, R. E., Madigan, M. T., Bauer, C. E., Eds.; Kluwer Academic Publishers: Dordrecht, The Netherlands, 1995.
(12) Bullough, P. A.; Qian, P.; Hunter, C. N. Reaction Center-Light-Harvesting Core Complexes of Purple Bacteria. In *The Purple Phototrophic Bacteria*; Hunter, C. N., Daldal, F., Thurnauer, M. C., Beatty, J. T., Eds.; Springer: Dordrecht, The Netherlands, 2009.
(13) Jungas, C.; Ranck, J. L.; Rigaud, J. L.; Joliot, P.; Vermeglio, A. *EMBO J.* **1999**, *18*, 534−542.
(14) Şener, M.; Hsin, J.; Trabuco, L. G.; Villa, E.; Qian, P.; Hunter, C. N.; Schulten, K. *Chem. Phys.* **2009**, *357*, 188−197.
(15) Walz, T.; Jamieson, S. J.; Bowers, C. M.; Bullough, P. A.; Hunter, C. N. *J. Mol. Biol.* **1998**, *282*, 833−845.
(16) Adams, P. G.; Hunter, C. N. *Biochim. Biophys. Acta Bioenerg.* **2012**, *1817*, 1616−1627.
(17) Şener, M.; Strümpfer, J.; Timney, J. A.; Freiberg, A.; Hunter, C. N.; Schulten, K. *Biophys. J.* **2010**, *99*, 67−75.
(18) Freiberg, A. Coupling of antennas to reaction centers. In *Anoxygenic Photosynthetic Bacteria*; Blankenship, R. E., Madigan, M. T., Bauer, C. E., Eds.; Kluwer Academic Publishers: Dordrecht, The Netherlands, 1995; Vol. 2, pp 385−398.
(19) Vredenberg, W. J.; Duysens, L. N. M. *Nature* **1963**, *197*, 355−357.
(20) McDermott, G.; Prince, S. M.; Freer, A. A.; Hawthornthwaite-Lawless, A. M.; Papiz, M. Z.; Cogdell, R. J.; Isaacs, N. W. *Nature* **1995**, *374*, 517−521.
(21) Sundström, V.; Pullerits, T.; van Grondelle, R. *J. Phys. Chem. B* **1999**, *103*, 2327−2346.
(22) Sumi, H. *Chem. Rec.* **2001**, *1*, 480−493.
(23) Hu, X.; Ritz, T.; Damjanovic, A.; Autenrieth, F.; Schulten, K. *Q. Rev. Biophys.* **2002**, *35*, 1−62.
(24) Novoderezhkin, V. I.; van Grondelle, R. *Phys. Chem. Chem. Phys.* **2010**, *12*, 7352−7365.
(25) Freiberg, A.; Trinkunas, G. Unraveling the hidden nature of antenna excitations. In *Photosynthesis in Silico. Understanding Complexity From Molecules to Ecosystems*; Laisk, A., Nedbal, L., Govindjee, Eds.; Springer: Heidelberg, 2009; pp 55−82.
(26) Reddy, N. R. S.; Small, G. J.; Seibert, M.; Picorel, R. *Chem. Phys. Lett.* **1991**, *181*, 391−399.
(27) Timpmann, K.; Freiberg, A.; Godik, V. I. *Chem. Phys. Lett.* **1991**, *182*, 617−22.
(28) Freiberg, A.; Rätsep, M.; Timpmann, K.; Trinkunas, G.; Woodbury, N. W. *J. Phys. Chem. B* **2003**, *107*, 11510−11519.
(29) Freiberg, A.; Rätsep, M.; Timpmann, K.; Trinkunas, G. *Chem. Phys.* **2009**, *357*, 102−112.
(30) Toyozawa, Y. *Optical Processes in Solids*; Cambridge University Press: Cambridge, U.K., 2003.
(31) Emin, D.; Holstein, T. *Phys. Rev. Lett.* **1976**, *36*, 323−326.
(32) Trinkunas, G.; Freiberg, A. *J. Lumin.* **2005**, *112*, 420−423.
(33) Kunz, R.; Timpmann, K.; Southall, J.; Cogdell, R. J.; Freiberg, A.; Köhler, J. *J. Phys. Chem. B* **2012**, *116*, 11017−11023.
(34) Pajusalu, M.; Rätsep, M.; Trinkunas, G.; Freiberg, A. *ChemPhysChem* **2011**, *12*, 634−644.
(35) Timpmann, K.; Trinkunas, G.; Olsen, J. D.; Hunter, C. N.; Freiberg, A. *Chem. Phys. Lett.* **2004**, *398*, 384−388.
(36) Trinkunas, G.; Freiberg, A. *J. Lumin.* **2006**, *119−120*, 105−110.
(37) Timpmann, K.; Trinkunas, G.; Qian, P.; Hunter, C. N.; Freiberg, A. *Chem. Phys. Lett.* **2005**, *414*, 359−363.
(38) Freiberg, A.; Timpmann, K.; Trinkunas, G. *Chem. Phys. Lett.* **2010**, *500*, 111−115.
(39) Dawkins, D. J.; Ferguson, L. A.; Cogdell, R. The structure of the "core" of the purple bacterial photosynthetic unit. In *Photosynthetic Light-Harvesting Systems: Organization and Function*; Scheer, H., Schneider, S., Eds.; Walter de Gruyter and Co.: Berlin and New York, 1988; pp 115−127.
(40) Freiberg, A.; Rätsep, M.; Timpmann, K. *Biochim. Biophys. Acta Bioenerg.* **2012**, *1817*, 1471−1482.
(41) Gall, A.; Sogaila, E.; Gulbinas, V.; Ilioaia, O.; Robert, B.; Valkunas, L. *Biochim. Biophys. Acta Bioenerg.* **2010**, *1797*, 1465−1469.
(42) Trinkunas, G.; Zerlauskiene, O.; Urbonienė, V.; Chmeliov, J.; Gall, A.; Robert, B.; Valkunas, L. *J. Phys. Chem. B* **2012**, *116*, 5192−5198.
(43) Freiberg, A.; Timpmann, K.; Lin, S.; Woodbury, N. W. *J. Phys. Chem. B* **1998**, *102*, 10974−10982.
(44) Freiberg, A.; Jackson, J. A.; Lin, S.; Woodbury, N. W. *J. Phys. Chem. A* **1998**, *102*, 4372−4380.
(45) Bahatyrova, S.; Frese, R. N.; Siebert, C. A.; Olsen, J. D.; van der Werf, K. O.; van Grondelle, R.; Niederman, R. A.; Bullough, P. A.; Otto, C.; Hunter, C. N. *Nature* **2004**, *430*, 1058−1062.
(46) Freiberg, A.; Godik, V. I.; Pullerits, T.; Timpmann, K. E. *Chem. Phys.* **1988**, *128*, 227−235.
(47) Freiberg, A.; Godik, V. I.; Pullerits, T.; Timpmann, K. *Biochim. Biophys. Acta* **1989**, *973*, 93−104.
(48) Timpmann, K.; Woodbury, N. W.; Freiberg, A. *J. Phys. Chem. B* **2000**, *104*, 9769−9771.
(49) Borisov, A. Y.; Freiberg, A. M.; Godik, V. I.; Rebane, K.; Timpmann, K. *Biochim. Biophys. Acta* **1985**, *807*, 221−229.
(50) Timpmann, K.; Freiberg, A.; Sundström, V. *Chem. Phys.* **1995**, *194*, 275−283.
(51) Scholes, G. D.; Fleming, G. R. *J. Phys. Chem. B* **2000**, *104*, 1854−1868.
(52) Georgakopoulou, S.; Frese, R. N.; Johnson, E.; Koolhaas, C.; Cogdell, R. J.; van Grondelle, R.; van der Zwan, G. *Biophys. J.* **2002**, *82*, 2184−2197.
(53) Harel, E. *J. Chem. Phys.* **2012**, *136*, 174104.
(54) Huo, P.; Coker, D. F. *J. Chem. Phys.* **2012**, *136*, 115102.
(55) Galve, F.; Pachon, L. A.; Zueco, D. *Phys. Rev. Lett.* **2010**, *105*, 180501.